Scopus

Documents

1)   Nesterenko, T.G., Koleda, A.N., Barbin, E.S.
   Integrated microelectromechanical gyroscope under shock loads
   (2018) IOP Conference Series: Materials Science and Engineering, 289 (1), art. no. 012003, .

1)   https://www.scopus.com/inward/record.uri?eid=2-s2.0-85041079633&doi=10.1088%2f1757-899X%2f289%2f1%2f012003&partn
   DOI: 10.1088/1757-899X/289/1/012003

   Document Type: Conference Paper
   Publication Stage: Final
   Access Type: Open Access
   Source: Scopus

PAPER • OPEN ACCESS

Integrated microelectromechanical gyroscope under shock loads

To cite this article: T G Nesterenko *et al* 2018 *IOP Conf. Ser.: Mater. Sci. Eng.* **289** 012003

View the article online for updates and enhancements.

IOP ebooks™

Bringing you innovative digital publishing with leading voices to create your essential collection of books in STEM research.

Start exploring the collection - download the first chapter of every title for free.

Integrated microelectromechanical gyroscope under shock loads

T G Nesterenko[1], A N Koleda[2] and E S Barbin[3]

[1] Associate Professor, National Research Tomsk Polytechnic University, Tomsk, Russia

[2] Assistant, National Research Tomsk Polytechnic University, Tomsk, Russia

[3] Engineer, National Research Tomsk Polytechnic University, Tomsk, Russia

E-mail: ntg@tpu.ru

Abstract. The paper presents a new design of a shock-proof two-axis microelectromechanical gyroscope. Without stoppers, the shock load enables the interaction between the silicon sensor elements. Stoppers were installed in the gyroscope to prevent the contact interaction between electrodes and spring elements with fixed part of the sensor. The contact of stoppers occurs along the plane, thereby preventing the system from serious contact stresses. The shock resistance of the gyroscope is improved by the increase in its eigenfrequency at which the contact interaction does not occur. It is shown that the shock load directed along one axis does not virtually cause the movement of sensing elements along the crosswise axes. Maximum stresses observed in the proposed gyroscope at any loading direction do not exceed the value allowable for silicon.

1. Introduction

The recent years have seen scientific and technical and technological advances in microsystems engineering which are widely used in different fields of information technology including microsensors. Microelectromechanical systems (MEMS) are one of the most prospective trends in modern electronics. MEMS technology utilizes methods similar to those applied in chipping technology allowing to create systems during the integration process, which possess mechanical electrochemical, optical and electronic properties and sizes comparable with ordinary integrated circuits.

Gyroscopes and accelerometers are the most popular MEMS devices suitable for numerous applications of consumer and engineering electronics, namely: car's safety systems, navigation and orientation of automotive vehicles, monitoring facilities, non-destructive testing monitoring systems for buildings, industrial facility platform stabilization, medical monitoring devices, oil and gas extraction devices [1–4].

The dissemination of MEMS sensor in all areas of the life is achieved largely by MEMS technology which has become popular and is not expensive. The process of MEMS development and production requires the extensive infrastructure starting from specialized tools and ending with production capabilities which provide specific procedures such as deep silicon etching.

A rapid development of MEMS sensors is conditioned by the following advantages [4–8]:

Microminiature circuits. Microcircuit technology allows producing micromechanical and optical assemblies with considerably less size than it is possible by using traditional technologies.

High operability. The incorporation of microcircuits and sensors, processing circuits and actuating device in one structure allows creating complex comprehensible systems in a miniature housing.

High production efficiency and repeatability. MEMS manufacturing mostly utilizes tried out and controlled operating procedures, which produce products with desired parameters.

Narrow spread of parameters within the product. The production of components in the single technological cycle allows obtaining virtually indistinguishable parameters for the same components.

High-performance operability. Electronics as well as electric communication channels made by the integrated technology and having small sizes allow improving such parameters as operating frequency, signal-to-noise ratio, and others.

Low cost mass production.

At the same time, there is a number of problems and weak points connected with the sensor operation. Operating conditions for MEMS include strong vibrations and impacts. In order for MEMS sensors to be used on mobile objects under ultrahigh inertial loads, the strength analysis is required for the gyroscope structure and conservation of its metrological characteristics [9–15].

The main goal of this paper is to analyse the shock load on the two-axis MEMS gyroscope.

2. Configuration and operation principle

Microelectromechanical (MEMS) gyroscopes are devices that measure angular velocity of various objects. The proposed two-axis MEMS gyroscope comprises the electronic module and the silicon sensor, general configuration of which is illustrated in Figure 1. The silicon sensor converts the input signal (angular velocity) into the electric signal which is then processed by the electronic module to obtain output information.
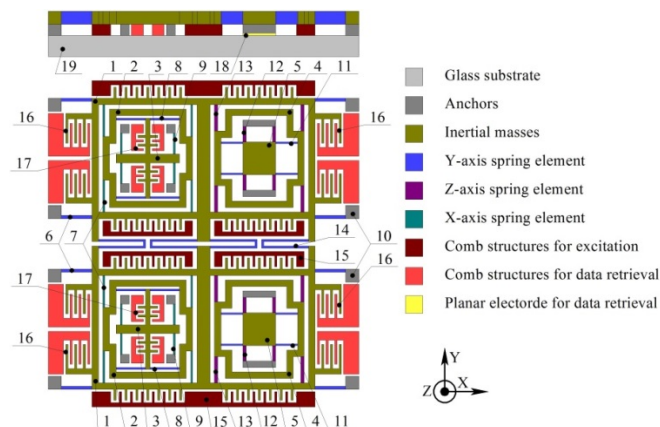

Figure 1. Configuration of MEMS gyroscope silicon sensor: *1* – frames; *2, 4* – decoupling frames; *3, 5* – inertial mass; *6, 8, 11, 14* – *Y*-axis spring elements; *7, 9* – *X*-axis spring elements; *10* – anchors; *12, 13* – *Z*-axis spring elements; *15* – comb drive actuator; *16* – comb structure for data retrieval along *Y*-axis; *17* – comb structure for data retrieval along *X*-axis; *18* – planar electrodes for data retrieval along *Z*-axis; *19* – glass substrate.

This gyroscope measures angular velocities Ω_x and Ω_z around *X*- and *Z*-axes, respectively. Its operation principle is based on the Coriolis effect. The gyroscope induces antiphase primary oscillations of frames (Figure 1) due to electrostatic forces created by the comb drive actuators. The displacement amplitudes of appeared secondary oscillations of inertial masses are proportional to Ω_x and Ω_z angular velocities.

3. Shock loads

The shock load analysis aims at the determination of deformations and mechanical stresses arising in micromechanical elements. The shock load causes the oscillations of the mechanical structure of the

silicon sensor. Shock loads are characterized by the acceleration rate, shock duration, and shock pulse waveform.

During the operation, MEMS gyroscope under the shock load should maintain the shock resistance both in on and off conditions and also restore their normal operation after this load. The requirements for operability and conservation of metrological characteristics are not usually regulated.

The structural design of the silicon sensor should be anticipated by the analysis of occurring stresses and the identification of more vulnerable stress locations. The spring element of the silicon sensor is the most vulnerable to the shock load because its rigidity is considerably lower than that of the entire structure. Shock-induced stresses in the spring element should not exceed those allowable for the sensor material.

According to the fourth failure hypothesis [16] of material, the amount of specific potential energy of distortion stored by the deformed element is accepted as the strength criterion. The dangerous condition is experienced when the specific potential energy of distortion achieves its limiting value which is determined by simple tension and compression tests. Hence, the stress condition is defined by

$$\sigma_{eq} \leq [\sigma_{lim}] \tag{1}$$

where σ_{lim} is the limit stress of material. The equivalent stress σ_{eq} shown in Figure 2 is calculated as

$$\sigma_{eq} = \sqrt{\frac{(\sigma_1 - \sigma_2)^2 + (\sigma_2 - \sigma_3)^2 + (\sigma_1 - \sigma_3)^2}{2}} \tag{2}$$

where $\sigma_1, \sigma_2, \sigma_3$ are primary stresses in the structure.

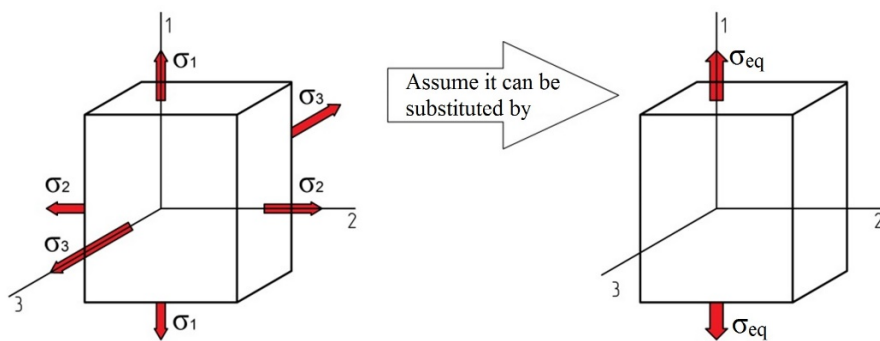Figure 2 illustrates the schematic layout of the specific potential energy of distortion.

Figure 2. Schematic layout of specific potential energy of distortion.

Let us assume that the shock pulse waveform is a sinusoidal half wave with 3500 Hz amplitude and 500 μs length. The shock load can be either long- or short-term. Its behavior depends on the eigenfrequency ω_0 of the system oscillations and is driven by the shock load.

The relative movement of sensing elements during and after the shock load is the product of the eigenfrequency and duration of the shock pulse $\omega_0 \cdot \tau$. For the proposed gyroscope, $\omega_0 \cdot \tau \approx 33.4$ on each axis, *i.e.* less than unity. So, the shock is long-term, and the movement of sensing elements induced by shock accelerations can be considered as a quasi-static.

In addition to the deformation of spring elements, the contact velocity of electrodes represents a threat to the sensor material. The material fracture due to shock can occur if the shock speed increases the value of [16, 17]

$$V_{im} = \frac{\sigma_{lim}}{\sqrt{E \cdot \rho}}, \tag{3}$$

where ρ is the silicon density; E is the Young's modulus.

The allowable shock load is 25 m/s in <110> direction of the silicon single crystal. The shock load is $V_0 = W/\omega_0$ for the considered long-term shock, where W is the shock acceleration at the time of contact. The first three eigenfrequencies of the gyroscope are observed in the vicinity of 10 kHz. As the shock speed is 0.51 m/s, the fracture of material does not occur when contacting.

However, the movement of sensing elements at certain shock parameters exceeds the values of allowable gaps. Thus, the configuration of the silicon sensor implies the contact interaction between its elements. Figures 3–5 contain the simulation plots of the shock load applied to the gyroscope while in operation, however, without the contact interaction.
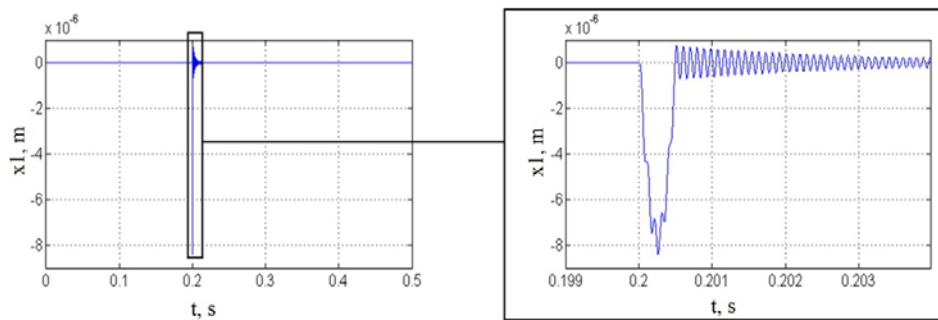

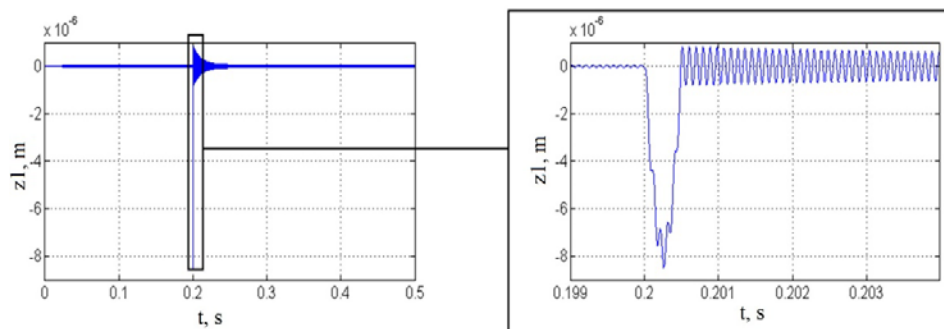**Figure 3.** Computer simulation of shock-induced movement of sensing elements along *X*-axis.

Figure 4. Computer simulation of shock-induced movement of sensing elements along *Z*-axis.
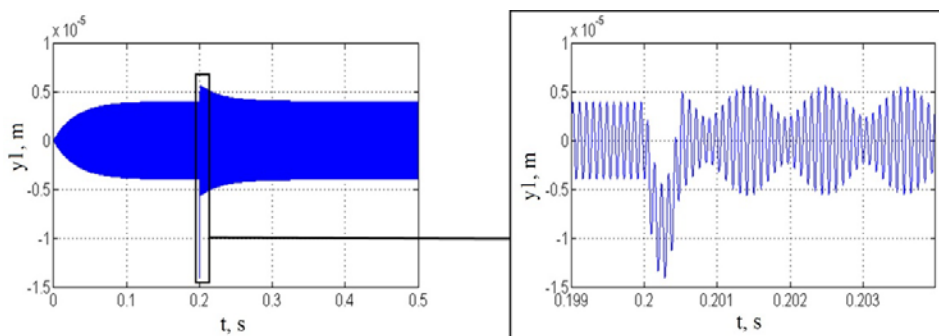

Figure 5. Computer simulation of shock-induced movement of sensing elements along *Y*-axis.

The sensing elements can move to a following distances during the shock loading if no limit is placed on their movement, namely: 9.5×10^{-6} m along *X*-axis; 9.2×10^{-6} m along *Y*-axis and 9.2×10^{-6} m along *Z*-axis. Minimum gaps between moving and fixed parts of the structure are several times less than these distances. So, the contact interaction is observed in both spring element and electrode structures, thereby leading to their fracture and the fracture of the electronic module due to the short-circuit failure.

In order to prevent the silicon sensor from the shock load, the gyroscope configuration is provided with stoppers depicted in Figure 6. These stoppers limit the movement of moving parts within 4 μm. Given that the gap width in comb electrodes is 5 μm, there is no any contact between them, whereas it is observed in places where the stoppers are located.
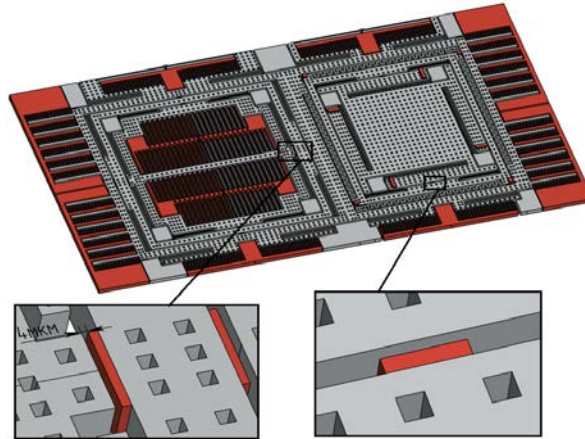

Figure 6. MEMS sensor configuration with stoppers.

The finite element method is used to analyze the contact interactions between the gyroscope structure and the stoppers. The possible directions of sensing element movement, movement of sensing elements before the contact, and occurred stresses are measured successively. This is illustrated in Figures 7–9.
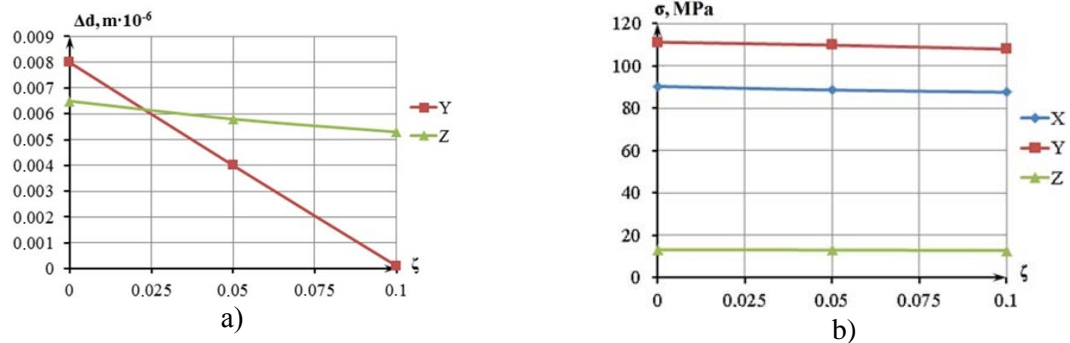

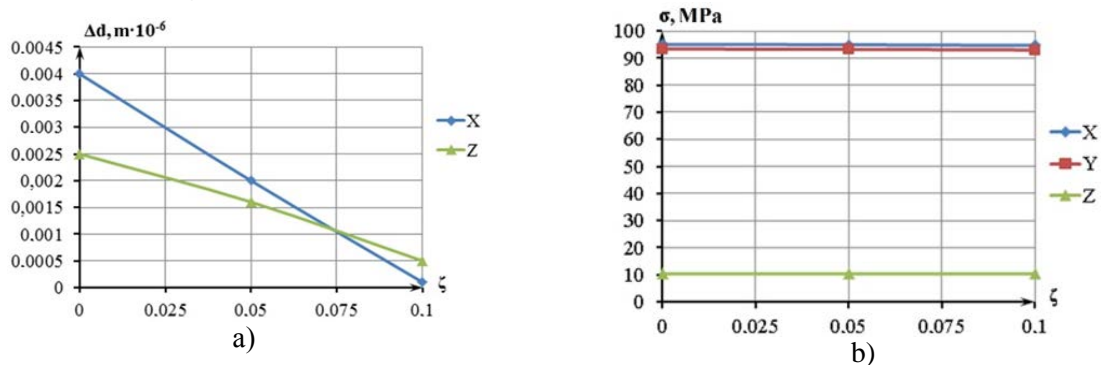**Figure 7.** Movements (a) and stresses (b) due to shock on *X*-axis.

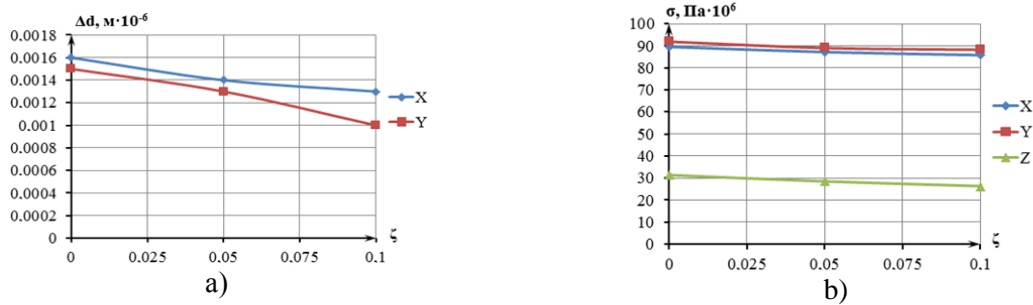**Figure 8.** Movements (*a*) and stresses (*b*) due to shock on *Y*-axis.

Figure 9. Movements (a) and stresses (b) due to shock on *Z*-axis.

As can be seen from these figures, the movement of sensing elements along the crosswise axes are less, and the occurred stresses are also less than their limit value.

4. Conclusions

In this paper, the authors proposed the shock-proof two-axis microelectromechanical gyroscope. It was shown that without stoppers, the shock load enabled the contact interaction between the different parts of the silicon sensor. Stoppers were installed in the gyroscope to prevent the contact interaction between electrodes and spring elements with fixed part of the sensor. The contact of stoppers occurred along the plane enabling it to prevent serious contact stresses. At the increased shock resistance caused by the increase in gyroscope eigenfrequency up to 13500 Hz the contact interaction did not occur.

It was shown that the shock load directed along one axis did not virtually cause the movement of sensing elements along the crosswise axes. Maximum stresses observed in the proposed gyroscope at any loading direction did not exceed the value allowable for silicon.

Acknowledgment

References

[1]   Butakov N A 2004 *International Journal of Open Information Technologies* **2** 2307–8162 (in Russian)

[2]   Georgy J, Noureldin A, Korenberg M J, Bayoumi M M 2010 *IEEE Transactions on Intelligent Transportation Systems* **11** 856–872 doi: 10.1109/TITS.2010.2052805

[3]   Lane N D, Miluzzo E, Lu H, Peebles D, Choudhury T, and Campbell A T 2010 *IEEE Communications Magazine* **48** 140–150 doi: 10.1109/MCOM.2010.5560598

[4]   Khan W Z, Xiang Y, Aalsalem M Y and Arshad Q 2013 *IEEE Communications Surveys and Tutorials* **15** 402–427 doi: 10.1109/SURV.2012.031412.00077

[5]   Furfie B 2010 *Engineering and Technology* **5** 34–35 doi: 10.1049/et.2010.0406

[6]   Neul R, Kehr K, Döring C, Götz S, Hauer J and Veith M 2007 *IEEE Sensors Journal* **7** 302–309 doi: 10.1109/JSEN.2006.888610

[7]   Or E M and Pundik D 2007 *IEEE Transactions on Consumer Electronics* **53** 1508–1512 doi: 10.1109/TCE.2007.4429245

[8]   Murari B 2003 *IEEE Micro* **23** 36–44 doi: 10.1109/MM.2003.1209465

[9]   Evstifeev M I, Eliseev D P, Rozentsvein D V and Chelpanov I B 2012 *Gyroscopy and Navigation* **3** 51–55 doi: 10.1134/S2075108712010063

[10] Sundaram S et al 2011 *Journal of Micromechanics and Microengineering* **21** 045022 doi: 10.1088/0960-1317/21/4/045022

[11] Naumann M, Dietze O, McNeil A, Mehner J and Daniel S 2013 *TRANSDUCERS and*

EUROSENSORS 2013 570–573 doi: 10.1109/Transducers.2013.6626830

[12]   Nekrasov Y A, Moiseev N V, Belyaev Y V, Pavlova S V, Lyukshonkov R G 2017 *Gyroscopy and Navigation* **8** 31–37 doi: 10.1134/S207510871604009X

[13]   Younis M I, Jordy D and Pitarresi J M 2007 *Journal of Microelectromechanical Systems* **16** 628–638 doi: 10.1109/JMEMS.2007.896701

[14]   Zhou J, Jiang T, Jiao J W and Wu M 2014 *Microsystem Technologies* **20** 137–144 doi: 10.1007/s00542-013-1833-9

[15]   Nesterenko T, Barbin E, Koleda A, Zorina E 2016 *International Siberian Conference on Control and Communications* 7491845 doi: 10.1109/SIBCON.2016.7491845

[16]   Fedosev V I 1979 *Strength of Materials* (Moskva: Nauka Press)

[17]   Starovoitov E I 2008 *Strength of Materials* (Moskva: Fizmatlit Press)